Supplementary Materials

3D Porous Copper Skeleton Supported Zinc Anode toward High Capacity and Long Cycle Life Zinc Ion Batteries

Zhuang Kang,[†] Changle Wu,[†] Liubing Dong,*[,†,§] Wenbao Liu,[†,‖] Jian Mou,[†] Jingwen Zhang,[†] Ziwen Chang,[†] Baozheng Jiang,[†,‡] Guoxiu Wang,*[,§] Feiyu Kang,[†,‖] and Chengjun Xu *[,†]

[†]Shenzhen Geim Graphene Center, Graduate School at Shenzhen, and [‡]Tsinghua-Berkeley Shenzhen Institute (TBSI), Tsinghua University, Shenzhen 518055, China

[§]Centre for Clean Energy Technology, University of Technology Sydney, Ultimo NSW 2007, Australia

[‖]State Key Laboratory of New Ceramics and Fine Processing, School of Materials Science and Engineering, Tsinghua University, Beijing 100084, China

*L. D. e-mail: dong1060@126.com.

*G. W. e-mail: guoxiu.wang@uts.edu.au.

*C. X. e-mail: vivaxuchengjun@163.com.

Totals – 20 pages, 16 figures, and 2 tables

Table S1. The specific capacity of several kinds of cathodes

Cathode	Capacity	Test condition (current density; electrolyte)	Ref.
Mo_6S_8	134 mAh g^{-1}	0.05 C; 0.1 M $ZnSO_4$	[S1]
Co_3O_4	162 mAh g^{-1}	1 A g^{-1}; 1 M KOH with 10×10^{-3} M $Zn(Ac)_2$	[S2]
Prussian blue analogs	60 mAh g^{-1}	0.3 A g^{-1}; 1 M Na_2SO_4 with 0.01 M H_2SO_4	[S3]
$Na_{0.33}V_2O_5$	367.1 mAh g^{-1}	0.1 A g^{-1}; 3 M $Zn(CH_3F_3SO_3)_2$	[S4]
V_2O_5	372 mAh g^{-1}	0.3 A g^{-1}; 3 M $Zn(CH_3F_3SO_3)_2$ with 0.1 M Vanadium sol	[S5]
MnO_2 nanosheet	364 mAh g^{-1}	0.1 A g^{-1}; 2 M $ZnSO_4$ with 0.5 M $MnSO_4$	Our work

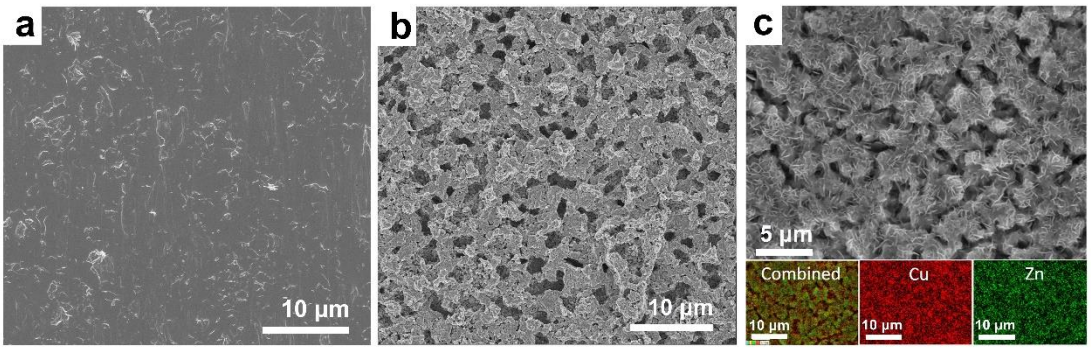

Figure S1. Top view SEM images of (a) original planar copper foil, (b) porous copper skeleton after chemical etching and (c) the porous copper skeleton after Zn-deposition and energy dispersive X-ray spectroscopy (EDS) mapping of Cu and Zn elements.

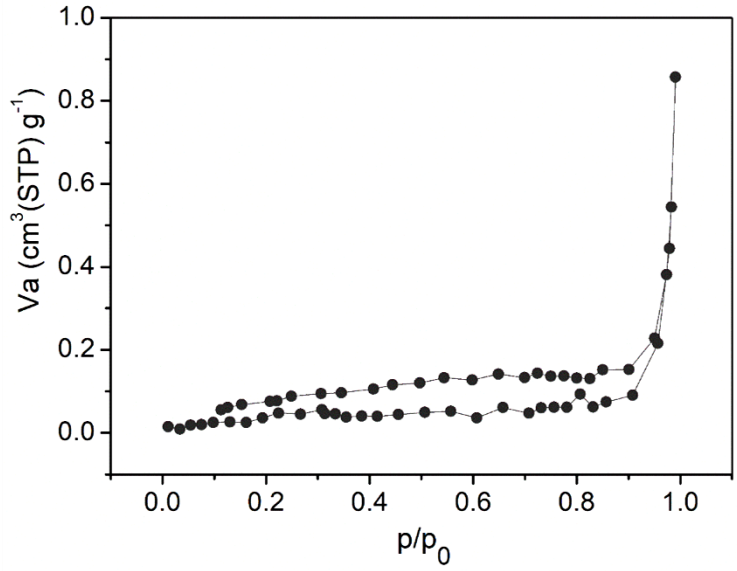

Figure S2. Nitrogen adsorption/desorption isotherm of porous copper skeleton.

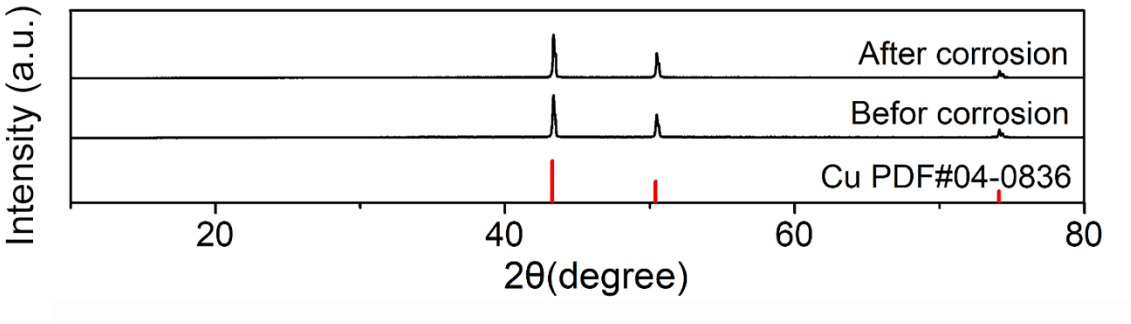

Figure S3. XRD patterns of copper before and after chemical etching.

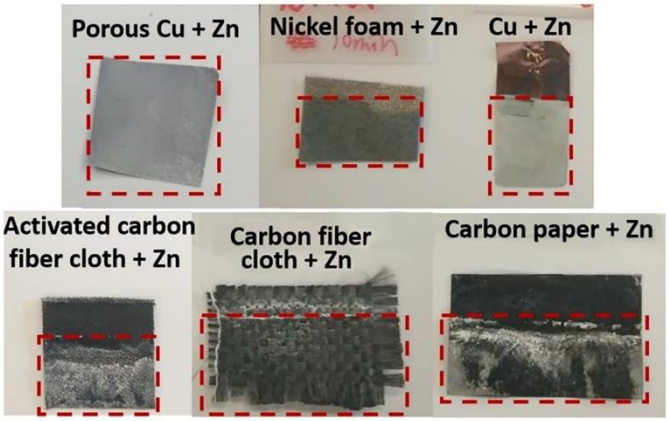

Figure S4. Zn deposition on different substrates. The area encircled by the red dotted rectangles in each image is the deposition area of Zn. Compared with metal substrates such as copper and nickel, electrodeposition of Zn on activated carbon fiber cloth, carbon fiber cloth and carbon paper often results in a less homogeneous macro-morphology.

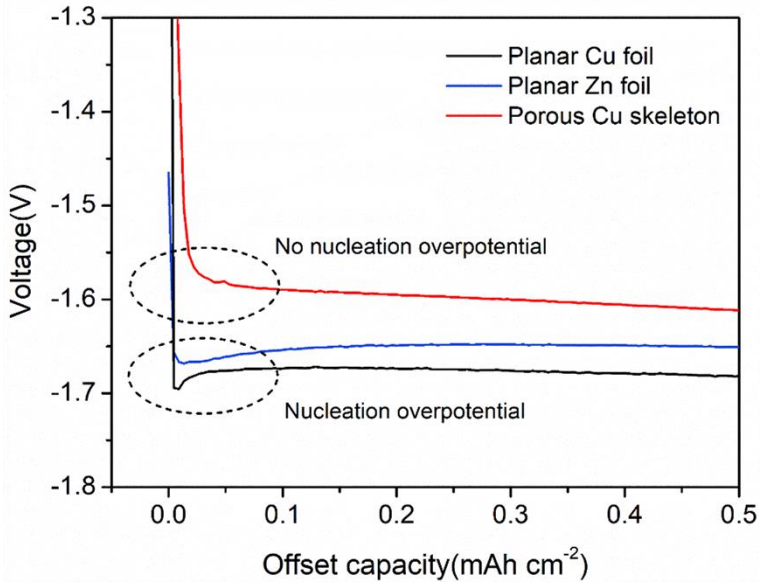

Figure S5. The electrodeposition curves of Zn on different substrates.

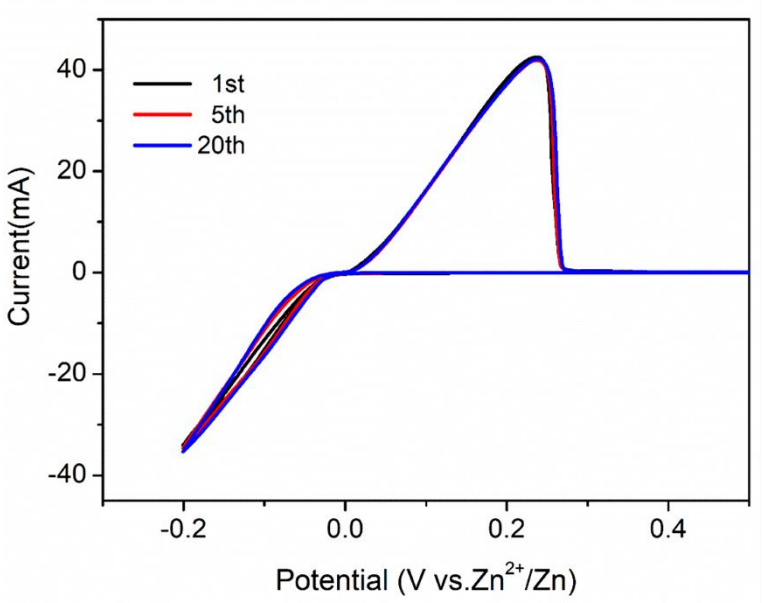

Figure S6. Cyclic voltammetry curves of 3D Zn anode at 0.5 mV s^{-1} in 2 M $ZnSO_4$ electrolyte.

Table S2. Accurate coulombic efficiency of Zn deposition/stripping. (symmetric cells, 2 M $ZnSO_4$ electrolyte, 1 mA cm^{-2}, 2 mAh cm^{-2})

Cycle number	Coulombic efficiency (%)	Cycle number	Coulombic efficiency (%)	Cycle number	Coulombic efficiency (%)
1	93.64	**23**	99.19	**45**	99.58
2	96.99	**24**	99.32	**46**	99.51
3	97.84	**25**	99.24	**47**	99.47
4	97.96	**26**	99.21	**48**	99.48
5	98.18	**27**	99.36	**49**	99.39
6	98.38	**28**	99.36	**50**	99.47
7	98.5	**29**	99.27	**51**	99.53
8	98.61	**30**	99.23	**52**	99.52
9	98.75	**31**	99.28	**53**	98.91
10	98.78	**32**	99.36	**54**	99.4
11	98.84	**33**	99.38	**55**	99.54
12	98.9	**34**	99.41	**56**	99.53
13	98.97	**35**	99.32	**57**	99.58
14	98.95	**36**	99.35	**58**	99.57
15	99.03	**37**	99.4	**59**	99.61
16	99.12	**38**	99.48	**60**	99.54
17	98.76	**39**	99.49	**61**	99.49
18	99.16	**40**	99.44	**62**	99.55
19	99.24	**41**	99.4	**63**	99.6
20	99.22	**42**	99.43	**64**	99.62
21	99.21	**43**	99.51	**65**	99.46
22	99.27	**44**	99.51	**66**	99.53

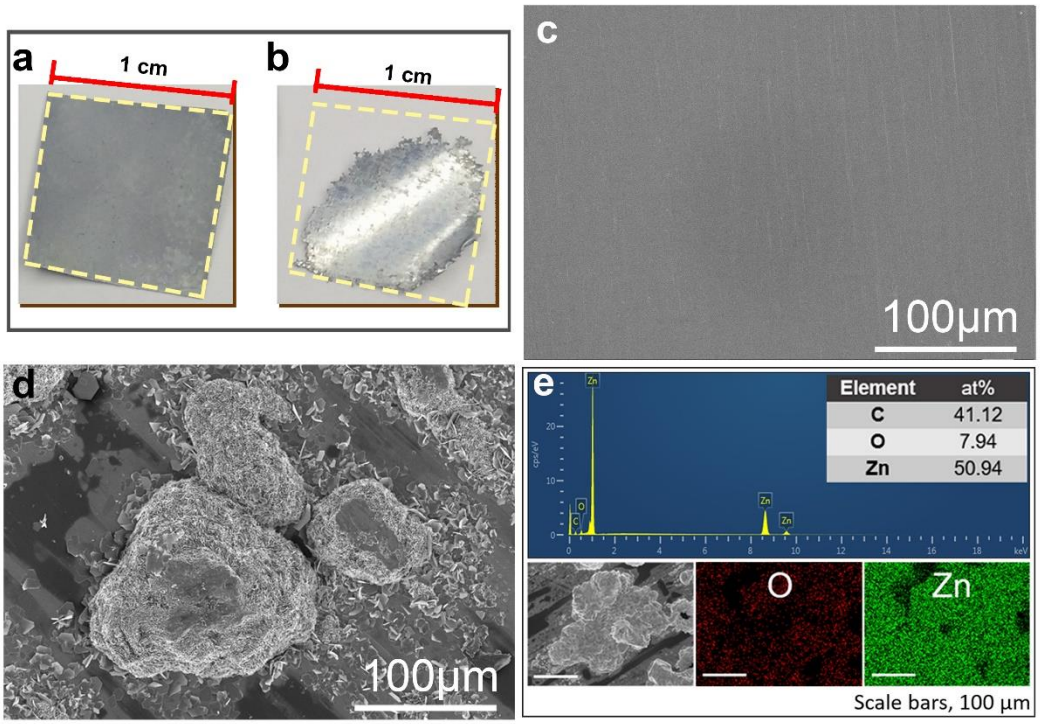

Figure S7. Digital photos of (a) our 3D Zn anode and (b) planar Zn foil anode after long-term charge/discharge cycles. Top view SEM images of (c) pristine planar Zn foil and (d) planar Zn foil anode after long-term charge/discharge cycles (large Zn protrusions appear). (e) EDS mapping of the sample in (d).

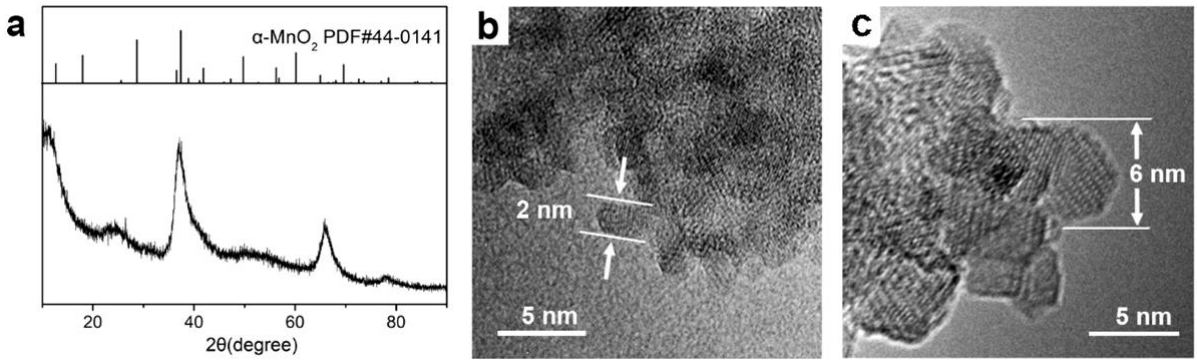

Figure S8. (a) XRD pattern and (b) (c) HRTEM images of MnO_2 powder. In the XRD pattern, four broad peaks appear at 12.8°, 25.7°, 37.5°, and 65.9°, corresponding to (110), (220), (211), and (002) planes of α-MnO_2, respectively. The formation of MnO_2 nanosheets by the redox reaction could be described as the following equation:

$$2MnO_4^- + 3SO_3^{2-} + H_2O \rightarrow 2MnO_2 + 3SO_4^{2-} + 2OH^-$$

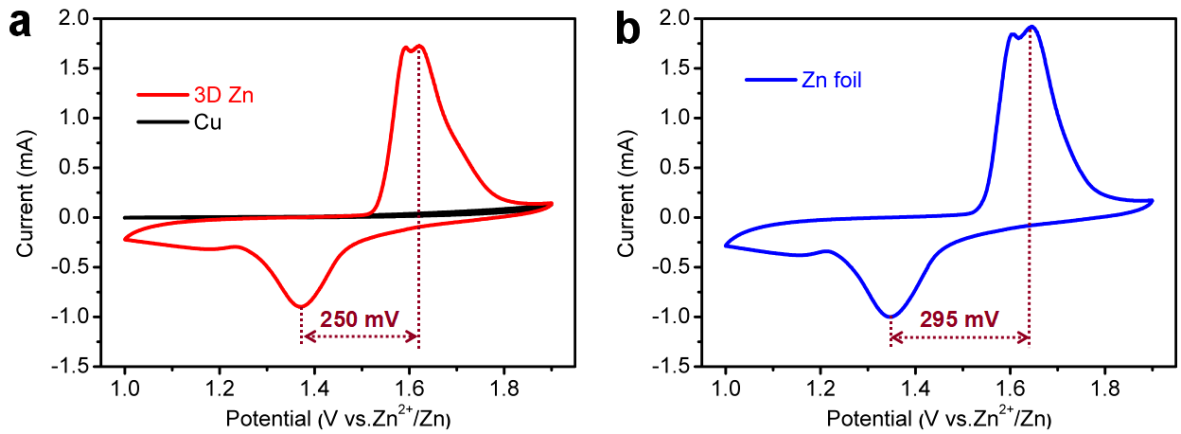

Figure S9. CV curves at 0.5 mV s^{-1} for the full cells with MnO_2 cathodes and different anodes in 2 M $ZnSO_4$ electrolyte: (a) 3D Zn anode; (b) planar Zn foil anode. For comparison, porous Cu skeleton (before Zn deposition) was directed used as anode.

z

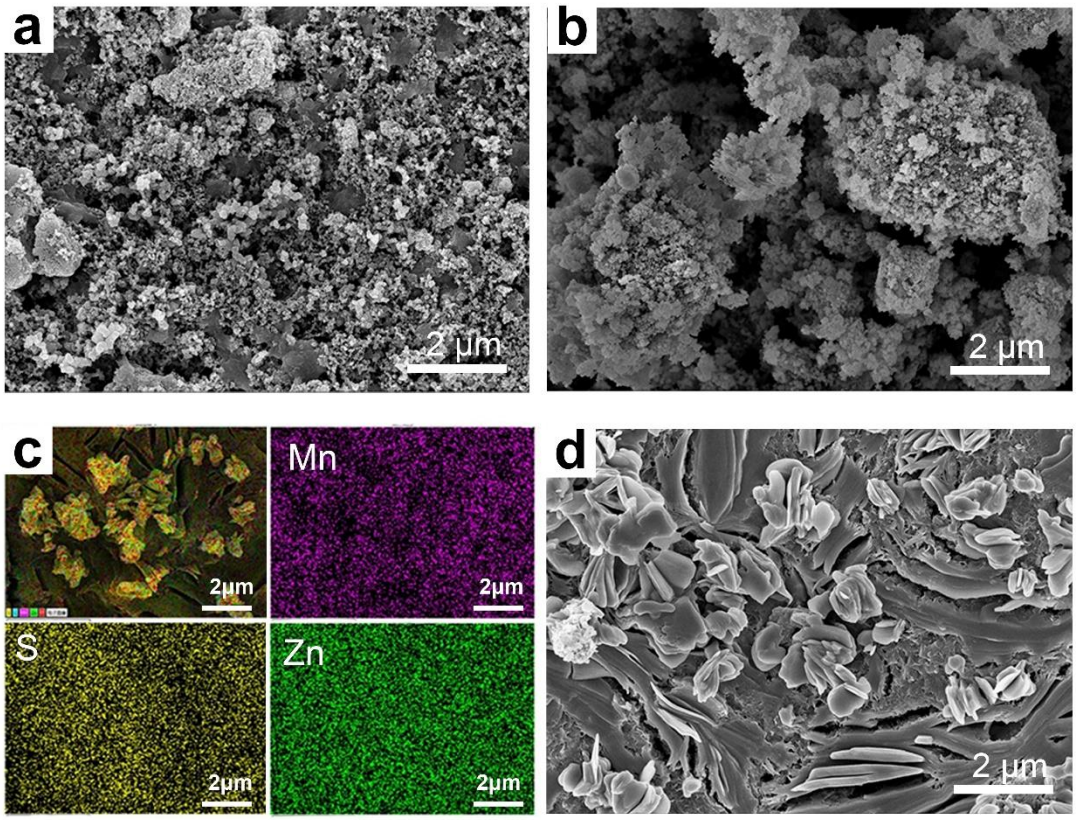

Figure S10. SEM images of a MnO_2 cathode in (a) original state and (b) fully charged to 1.9 V. (c) EDS mapping of a MnO_2 cathode in a fully discharged state. (d) SEM image of a MnO_2 cathode when the ZIB cell was fully discharged to 1.0 V.

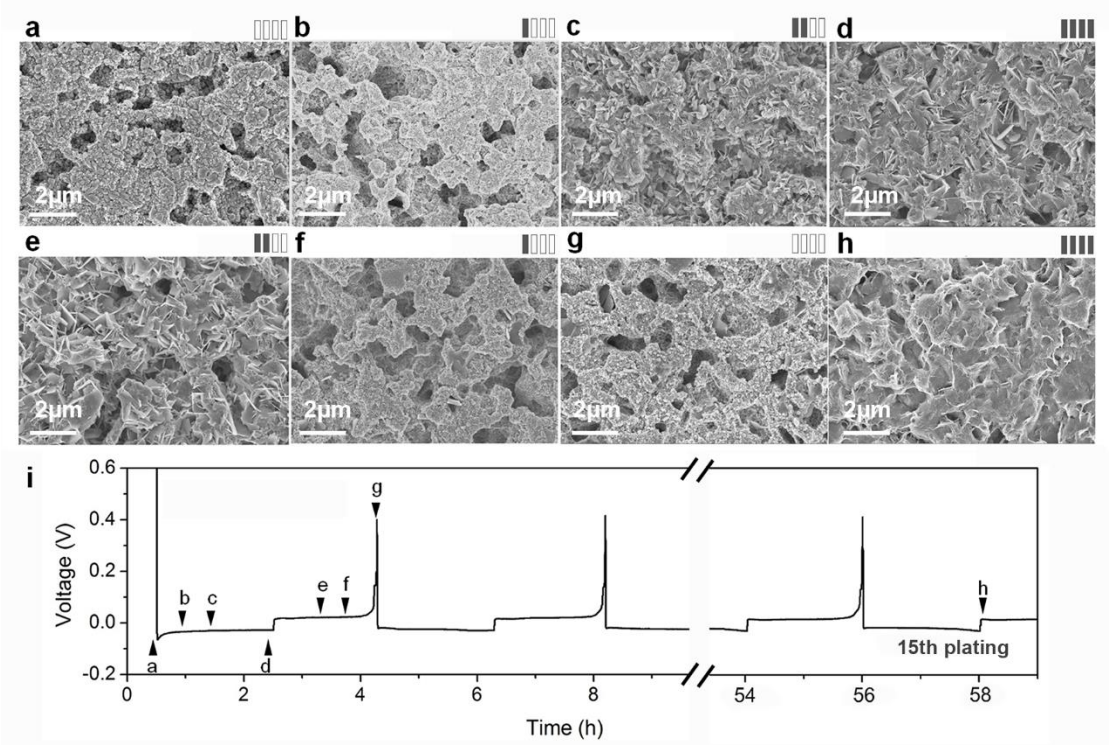

Figure S11. Morphology variations of 3D Zn electrodes at various Zn deposition or stripping amounts in electrolyte containing 2 M $ZnSO_4$ and 0.5 M $MnSO_4$. Top view SEM images of (a) porous copper skeleton, after depositing different amounts of Zn ─ (b) 0.5 mAh cm^{-2}, (c) 1 mAh cm^{-2}, and (d) 2 mAh cm^{-2} ─ and then stripping different amounts of Zn ─ (e) 1 mAh cm^{-2}, (f) 1.5 mAh cm^{-2}, and (g) 2 mAh cm^{-2}. (i) SEM image of the 3D Zn anode (with 2 mAh cm^{-2} of Zn) after repeated deposition/stripping for 15 cycles. The rectangle symbols show the amount of Zn metal in each image; each solid rectangle represents 0.5 mAh cm^{-2} of Zn. Zn deposition/stripping states (b–i) are indicated in (j) galvanostatic discharge/charge voltage profile at a current density of 1 mA cm^{-2} in 2 M $ZnSO_4$ electrolyte. The rectangle symbols show the amount of Zn metal in each image; each solid rectangle represents 0.5 mAh cm^{-2} of Zn. Zn deposition/stripping states (a–h) are indicated in (i) a galvanostatic discharge/charge profile at a current density of 1 mA cm^{-2}.

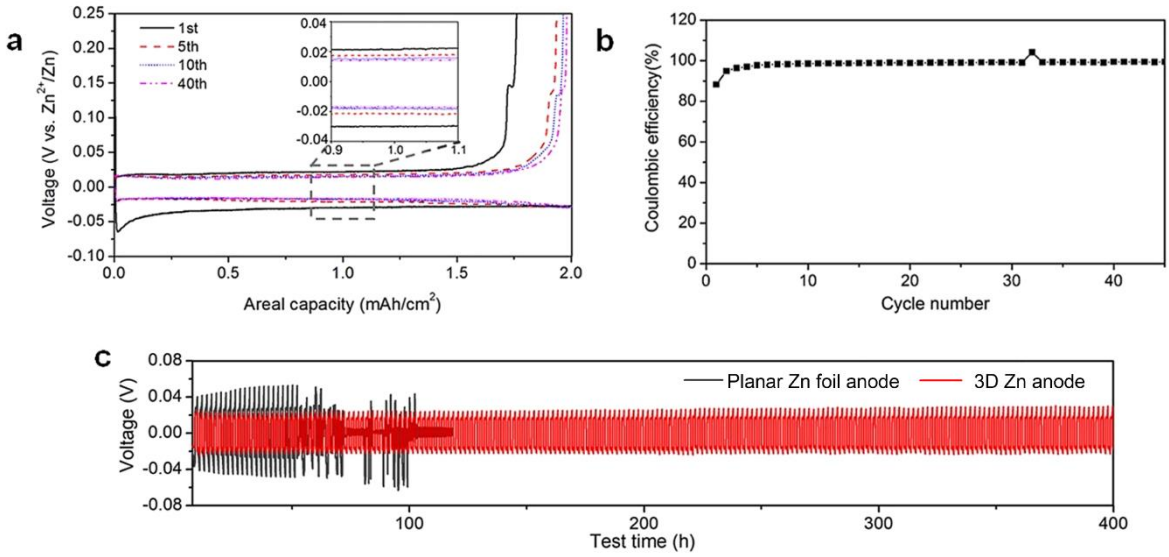

Figure S12. Electrochemical behaviors of symmetric cells with electrolyte containing 2 M $ZnSO_4$ and 0.5 M $MnSO_4$. (a) Discharge/charge voltage profiles with 1 mA cm^{-2} of Zn plating/stripping, and the inset enlarges the voltage profiles in the range of 0.9-1.1 mAh cm^{-2}; (b) CE values; (c) Cycling performance at a constant current of 0.5 mA cm^{-2}.

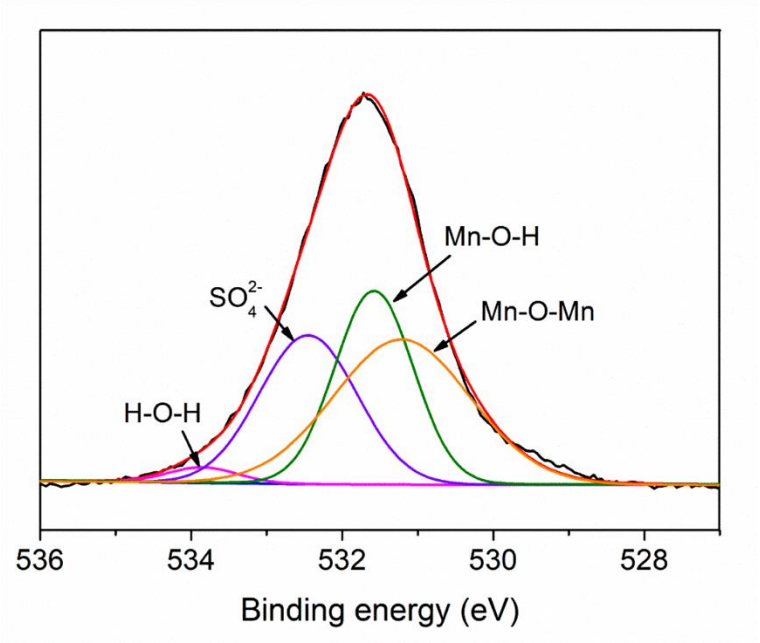

Figure S13. O 1s XPS spectra of a MnO_2 cathode in fully discharged state.

When the current densities and areal capacity raised to 2 mAh cm^{-2} (with Zn deposition of 6 mAh cm^{-2}), the result is shown in the **Figure S14**. 3D Zn anode is not stable and shows a large voltage hysteresis at about 40 h while short circuit damage to the planar Zn foil electrode-based cells occurs at about 40 h.

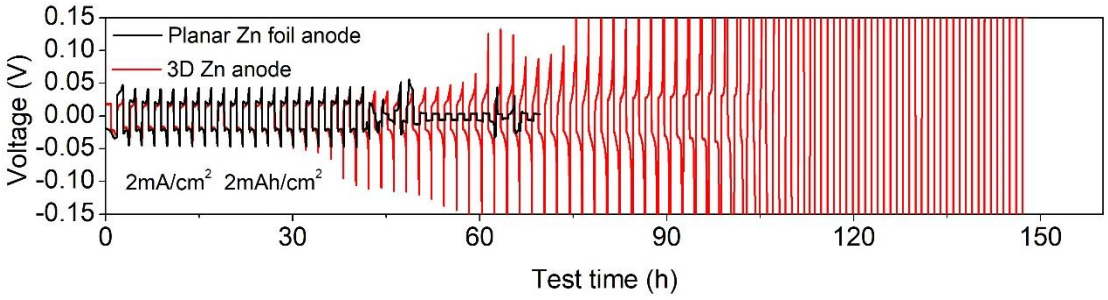

Figure S14. Cycling performance of symmetric cells with 2 M $ZnSO_4$ electrolyte. Discharge/charge voltage profiles of Zn plating/stripping when the current density is raised to 2 mA cm^{-2} and the areal capacity is 2 mAh cm^{-2}.

To accommodate the larger current density and area density, the total deposition amount of zinc in 3D Zn anode is increased to 20 mAh cm^{-2}. As the current density increases, the battery cycle stability decreases (**Figure S15**).

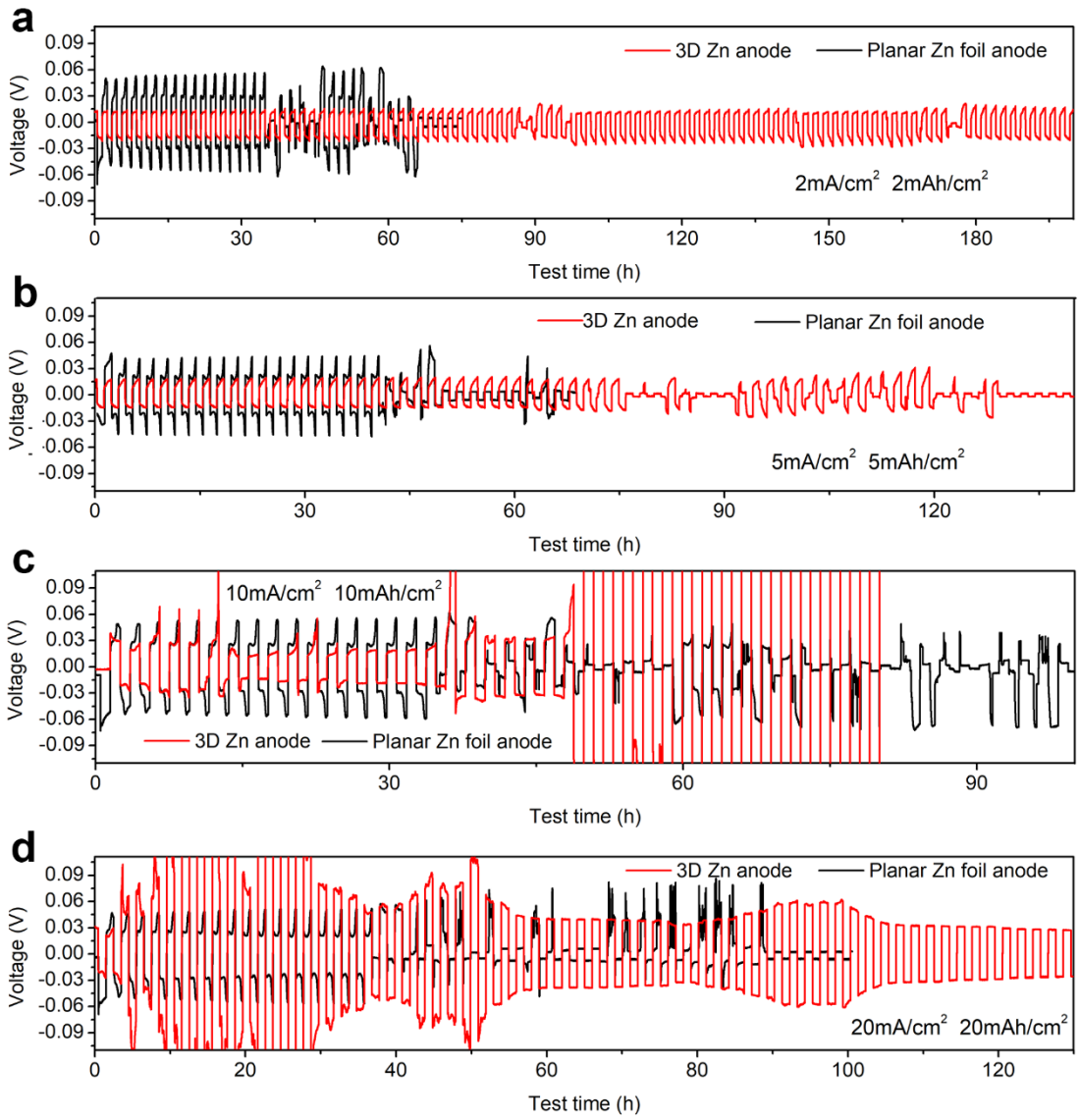

Figure S15. Cycling performance of symmetric cells with 2 M $ZnSO_4$ electrolyte. Discharge/charge voltage profiles of Zn plating/stripping when the current density is raised to (a) 2 mA cm^{-2}, (b) 5 mA cm^{-2}, (c) 10 mA cm^{-2}, and (d) 20 mA cm^{-2} and the areal capacity is accordingly increased to 2 mAh cm^{-2}, 5 mAh cm^{-2}, 10 mAh cm^{-2}, and 20 mAh cm^{-2}, while the total deposition amount of zinc in 3D Zn anode is 20 mAh cm^{-2}.

Unfortunately, the 3D porous Cu skeleton has a limited space capacity due to the thickness of the copper foil. When the deposition amount continues increase, the 3D structure is excessively been covered, and the influence of the 3D structure on the reaction process cannot be sufficiently exhibited, like providing space for dendrite growth. **Figure S16a** shows the schematic diagrams of Zn deposition/stripping processes on 3D Zn electrodes while the amount of zinc is too much. **Figure S16b** shows the EDS images of the 3D zinc (cross section) deposited at 20 mAh cm^{-2}.

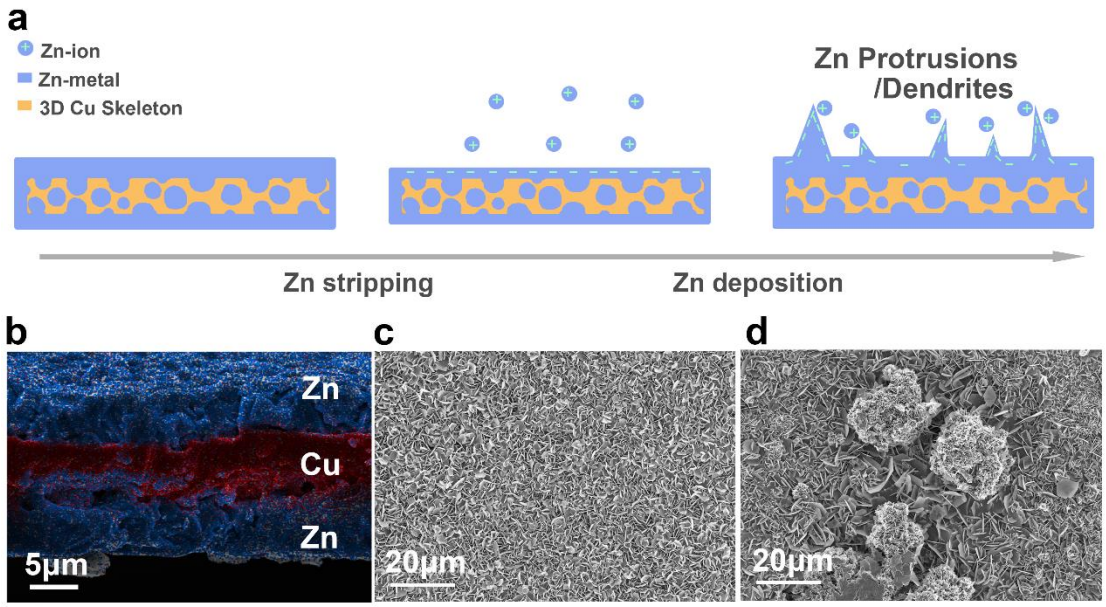

Figure S16. (a) Schematic diagrams of Zn deposition/stripping processes on 3D Zn electrodes while the amount of zinc is too much. (b) EDS images of sectional view of depositing 20 mAh cm^{-2} Zn on 3D Cu skeleton. (c) SEM image of Zn before cycling. (d) SEM image of Zn protrusions after cell failure (5 mA cm^{-2}, 5 mAh cm^{-2}).

REFERENCES

[S1] Chae, M. S.; Heo, J. W.; Lim, S.-C. & Hong, S.-T., Electrochemical zinc-ion intercalation properties and crystal structures of $ZnMo_6S_8$ and $Zn_2Mo_6S_8$ chevrel phases in aqueous electrolytes. *Inorg. Chem.* **2016**, 55, 3294-3301.

[S2] Wang, X.; Wang, F.; Wang, L.; Li, M.; Wang, Y.; Chen, B.; Zhu, Y.; Fu, L.; Zha, L.; Zhang, L.; Wu, Y. & Huang, W., An Aqueous Rechargeable Zn//Co_3O_4 Battery with High Energy Density and Good Cycling Behavior. *Adv Mater*. **2016**, 28, 4904-4911.

[S3] Gupta, T.; Kim, A.; Phadke, S.; Biswas, S.; Luong, T.; Hertzberg, B. J.; Chamoun, M.; Evans-Lutterodt, K. & Steingart, D. A., Improving the cycle life of a high-rate, high-potential aqueous dual-ion battery using hyper-dendritic zinc and copper hexacyanoferrate. *J. Power Sources* **2016**, 305, 22-29.

[S4] He, P.; Zhang, G.; Liao, X.; Yan, M.; Xu, X.; An, Q.; Liu, J. & Mai, L., Sodium Ion Stabilized Vanadium Oxide Nanowire Cathode for High-Performance Zinc-Ion Batteries. *Adv. Energy Mater.* **2018**, 8, 1702463.

[S5] Yan, M.; He, P.; Chen, Y.; Wang, S.; Wei, Q.; Zhao, K.; Xu, X.; An, Q.; Shuang, Y. & Shao, Y., Water-Lubricated Intercalation in $V_2O_5\cdot nH_2O$ for High-Capacity and High-Rate Aqueous Rechargeable Zinc Batteries. *Adv. Mater.* **2018**, 30, 1703725.